A New Approach for Absolute Calibration of a GNSS Receiver: Use of a Software-Defined Radio (SDR) Technique

P. Uhrich, F. Riedel, B. Chupin and M. Abgrall
LNE-SYRTE
Observatoire de Paris – Université PSL, CNRS, Sorbonne Université,
Paris, France
pierre.uhrich@obspm.fr

***Summary*—This paper describes a new approach for achieving absolute calibration of the receiver main unit of a GNSS station, based on the use of an affordable GNSS signal simulator and on a Software-Defined Radio (SDR) receiver for the measurement of the delay between the 1 PPS reference signal and the GNSS simulated signal code transition.**

Keywords—GNSS; Time Transfer; Calibration; SDR

I INTRODUCTION

Absolute calibration of delays of a Global Navigation Satellite System (GNSS) signal receiving station is required for any direct measurement of the GNSS signal against a local reference time scale. For example, this might concern the accurate determination of the offset between any local time scale and the GNSS broadcast prediction of Co-ordinated Universal Time (UTC). An absolute calibration of a GNSS station is usually computed separately for its three components: the antenna, the antenna cable and the receiver main unit [1,2,3]. During recent years, space agencies have published GNSS station absolute calibration results within combined uncertainties just below 1 ns [4]. LNE-SYRTE had formerly assessed the measurement of an antenna cable delay by different techniques within a combined uncertainty of about 300 ps [5]. An adapted anechoic chamber is also required for the antenna calibration [6]. In the following, we focus only on the receiver main unit calibration.

Absolute calibration of the receiver main unit of a GNSS station can be done by using a simulated signal. Among the issues to solve, the determination of the offset between the 1 Pulse Per Second (PPS) reference signal and one given transition of the simulated GNSS code is mandatory. There are different possibilities for such a delay measurement, depending on the equipment used. When a high level GNSS signal simulator is available, the noise of the simulated signal is low enough to allow for a determination within an uncertainty below 1 ns of this offset by using a high sampling rate oscilloscope. But the average cost of this kind of simulator makes it out of reach of a metrology laboratory like ours. If the remaining jitter of the simulated signal from an affordable simulator prevents a sub-ns determination of this offset with an oscilloscope, other measures are necessary. In Section II, we show the limits we could reach, after implementation of an adequate filtering of the signal. Another technique for measuring this delay accurately might be to collect a sufficient number of samples of the simulated signal and to digitally filter the expected code to achieve a sub-ns measurement against the reference 1 PPS [7]. But LNE-SYRTE is proposing here a new approach.

During the last few years indeed, the Two-Way Satellite Time and Frequency Transfer (TWSTFT) community developed the use of a Software-Defined Radio (SDR) technique, achieving a sub-ns combined uncertainty on remote clock comparisons [8]. We propose to start a similar development for GNSS calibration, by implementing an SDR receiver able to collect the data produced by the GNSS simulator. Provided a suitable software for carrier detection and code correlation is made available for SDR, a RINEX file is produced on receiver side, based on a received simulated GNSS signal. This should be related to the equivalent RINEX file of the signal transmitted by the simulator. The difference between these two RINEX files, corrected by the related cable and known equipment delays, might provide an offset between the transmitted GNSS simulated signal and the 1 PPS reference signal, if the 1 PPS reference is the same for both units. We show the experimental set-up of the selected equipment in Section III, together with the first results of measurements based on GPS C/A code signal in Section IV.

II LIMITS REACHED WHEN USING AN OSCILLOSCOPE

The GNSS signal simulator used by LNE-SYRTE is a GSG64 built by Spectracom Orolia. It can transmit C/A- or P-code GPS signals on both L1 = 1575.42 MHz and L2 = 1227.6 MHz carrier frequencies. In addition, it was recently upgraded to Galileo signals on both L1 and E5a = 1176.45 MHz carrier frequencies. Numerous configurations might be set for the simulated signal by merging signals of different types for a given constellation. In the rest of this paper, we limit the GNSS simulated signal to GPS C/A code on L1 carrier.

The first attempt to measure the offset between the 1 PPS reference signal and the chosen code transition of a GPS C/A simulated signal was made by using an oscilloscope. The set-up is simple: we put a cable between the GSG64 simulator and the oscilloscope, both instruments being connected to the UTC(OP)

1 PPS reference and to the UTC(OP) 10 MHz signal as stable source, UTC(OP) being the realization of UTC in Observatoire de Paris (OP) [9]. Figure 1 shows a picture of the oscilloscope screen with both signals on. One can notice that the simulated signal is extremely noisy, even preventing any proper identification of the code transition in the middle of the plot. The jitter is large and some amplitude modulation is also appearing on the simulated signal.

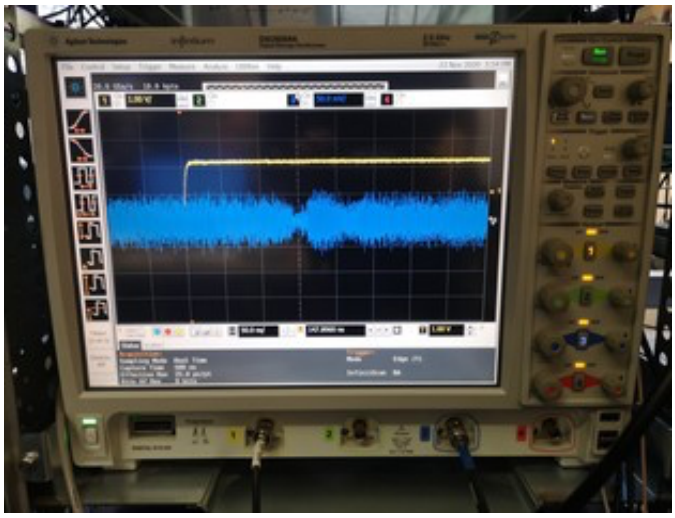

Fig. 1. Picture of an oscilloscope screen showing the 1 PPS reference signal (yellow) and the GPS L1 C/A simulated signal (blue).

We then added a bandpass filter of about 40 MHz around L1 carrier in-between the GSG64 output and the oscilloscope input. Of course, this is not a transparent move with respect to delay measurements, but the goal here was to properly see the code transition on the screen. Figure 2 shows the same signals as in Figure 1 after filtering: there is a clear improvement in the steadiness of the simulated signal, and the code transition is visible, together with the small additional amplitude modulation.

Zooming on the central part of the signal allows to focus on the code transition, as is show in Figure 3. Note that the horizontal scale is 5 ns/division. A sub-ns determination of the offset between the code zero-crossing and the 1 PPS reference signal seems possible by using an oscilloscope with this technique. But even assuming a sub-ns uncertainty on the transition position, it would then be mandatory to estimate the delay of the added bandpass filter, which would not be a trivial task. It would require the use of a Vector Network Analyzer (VNA) for achieving a sub-ns determination of such a delay. In addition, a much more complex filtering would be required for a comprehensive multi-carrier GNSS simulated signal, each adapted filter being designed for a given carrier frequency. With this technique, when merging all different code delay results, the resulting combined uncertainty might not be lower than 1 ns for the receiver main unit only, to be added to the other uncertainties for a complete station. For a sub-ns combined uncertainty target, it was worth exploring another technique like SDR.

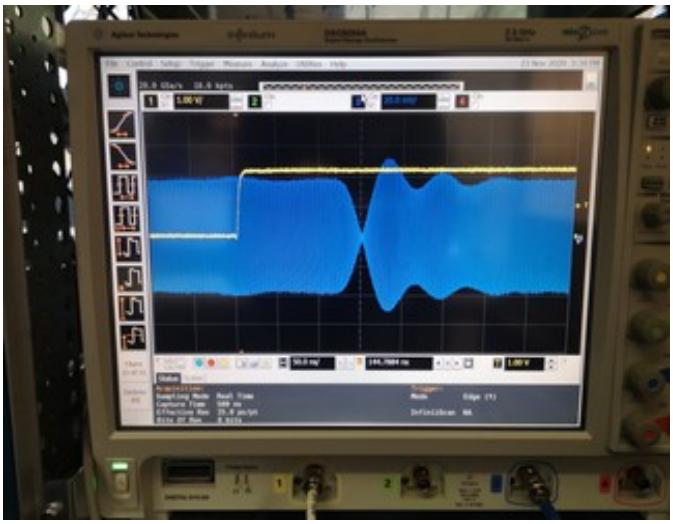

Fig. 2. Picture of an oscilloscope screen showing the 1 PPS reference signal (yellow) and the GPS L1 C/A simulated signal (blue) after implementation of a 40 MHz bandpass filter between the GSG64 and the oscilloscope.

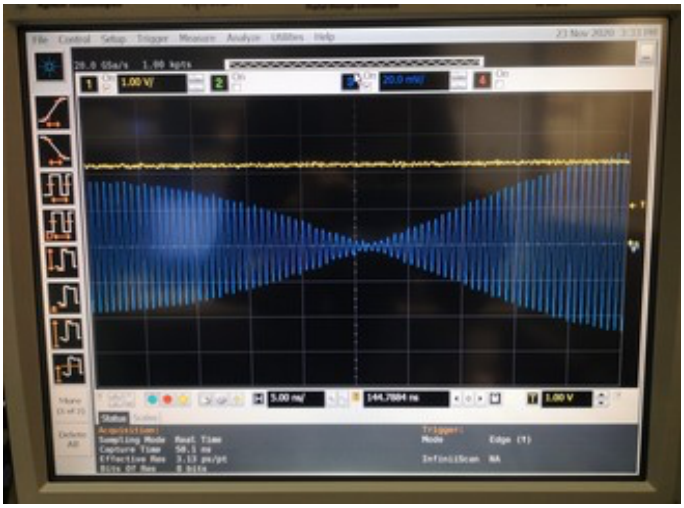

Fig. 3. Zoom in the code transition of Figure 3. The horizontal scale is 5 ns/division.

III SDR RECEIVER IMPLEMENTATION

LNE-SYRTE selected an SDR motherboard ETTUS X310, which is capable of receiving the L1 frequency directly, so no conversion would be necessary. It was bought together with a daughterboard UBX-160 that provides a bandwidth of 160 MHz, largely enough to cover both GPS C/A- and P-codes. But instead of using the SDR code already installed, we decided to implement a free software available from the internet which offers more GNSS codes implementation. The software called gnss-sdr was found the most suitable for our purpose [10].

The daughterboard implementation was however not straightforward. Figure 4 shows an overview of the inside of ETTUS X310 with the daughterboard UBX-160 installed on the slot A. Due to the daughterboard cooling, the internal short cables could not be connected to the out- and inputs labeled as A: the B connectors were used instead, but with LED A illuminated when in use. Moreover, the software to be used were UHD and GNU Radio. The challenge to match both software

versions with each other, in order to have the appropriate FPGA image loaded on the daughterboard required some efforts. To test the software implementation, a file is available in the gnss-sdr website for download [10], and the test was eventually successful.

Fig. 4. ETTUS X310 with installed UBX-160 daughterboard on slot A and internal cables leading to the ports labeled as B.

Figure 5 is describing the set-up of the connection between the GSG64 simulator and the ETTUS X310. The 10 MHz signal from UTC(OP) is provided to both instruments. The UTC(OP) 1 PPS is serving as input to the simulator. It could also be provided to the SDR receiver. But for calibration measurements, where the received RINEX files must be related to the transmitted ones, we use the 1 PPS output of the GSG64 as 1 PPS input to the SDR receiver: indeed, this GSG64 1 PPS output is supposed to be related to the reference latching point of the simulated signal. The rise time of this GSG64 1 PPS output is not as sharp as the UTC(OP) 1 PPS: about 8 ns from bottom to high level compared to 5 ns. Any jitter might have a potential impact on delay measurements.

A specific GSG64 scenario was created that transmits the L1 C/A simulated signal from 12 GPS satellites, the SDR being configured to receive up to 12 satellite signals. Figure 6 is showing the spectral signature of this simulated signal, which is appearing exactly as expected, when using a spectrum analyzer. However, it seems that only 4 to 7 satellites are tracked at once. A short series of measurements was carried out at the beginning of this experiment to determine an optimum power level. We eventually selected an amplifier AM-SA-0520 from MITEQ and a L1 bandpass filter TIC-1575.42B20-01 for a clean signal. All measurements discussed later were obtained with – 100 dBm power set at the simulator, which results in a typical power level of about – 50 dBm at the SDR input. However, although this was identified as an optimum input power, the locking process until a tracking of a certain number of satellites was achieved was varying in time from 30 s up to 5 min or more from repeated measurements for one given power level within the same set of parameters. We have no explanation yet.

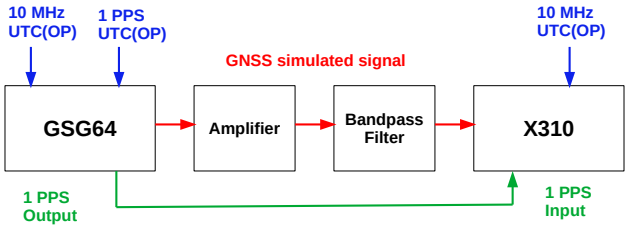

Fig. 5. Set-up for the measurement between Spectracom GSG64 ad ETTUS X310 for an optimum power level.

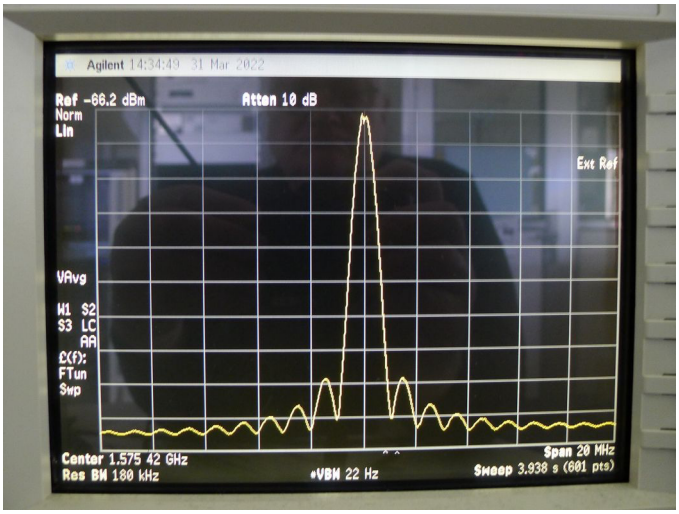

Fig. 6. Picture of a spectrum analyzer screen showing the simulated GPS L1 C/A signal at the output of the GSG64 simulator.

The files generated by the gnss-sdr software are RINEX2 or RINEX3 files of both observation and navigation types. For any measurement duration, one single file is created. For our processing, we had then to split these files from days of measurements into daily RINEX files, and to adapt the starting time in the header of the observation files together with the virtual antenna coordinates. To synchronize the simulated signal on UTC(OP), there are two different ways with the GSG64: either by pushing a «hold» button on the front panel of the instrument or remotely via a Studio View web interface. We noted however that there were differences in the daily files between both options, all other parameters unchanged. This is unexplained yet.

IV FIRST MEASUREMENT RESULTS WITH C/A GPS CODE

With the set-up in Figure 5, five series of measurements have been carried out with an equivalent scenario length of 3 d in terms of resulting RINEX files. One of these measurements was carried out with a power level 10 dB higher than the rest. In addition, three series of 3 d measurements have also been carried

out by using the 1 PPS UTC(OP) as input to SDR instead of the 1 PPS output of the GSG64.

At first, the SDR results are compared with each other by computing the Common-Views (CV) between one of the SDR measurements and the rest, after transformation of all RINEX files into 30 s sampled CGGTTS files. The SDR reference was noted s1L2 according to: “s” for SDR, “1” for 2021, “L” for December and “2” as second set of measurements for this month. We observed that he CV results are between -0.4 and 9.7 ms, 0.084 ms being the smallest. This is clearly much more than expected, and moreover, despite the scenario staying the same, the CV results are never identical. Noting that the 1 PPS output of the GSG64 is only available after the scenario start, this might be depending on the internal synchronization of the SDR, which might be related to an unknown trigger level and some jitter in the input signal. In addition, there are jumps and gaps in the data, never at the same place. In some cases, there seem to be an unexplained additional pattern between different data sets.

Figure 7 shows a typical CV plot between s1L2 and s1L3 (the third set of data in December 2021) with a few ms arbitray offset subtracted for better visibility. There is some transient term at the start, followed by some noisy signal with gaps, including the above-mentioned pattern. On the other hand, Figure 8 is showing the best CV we obtained between s1L2 and s1L1 (the first set of data in December 2021), with an arbitrary offset subtracted too: the CV are steady and the peak to peak is below 2 ns.

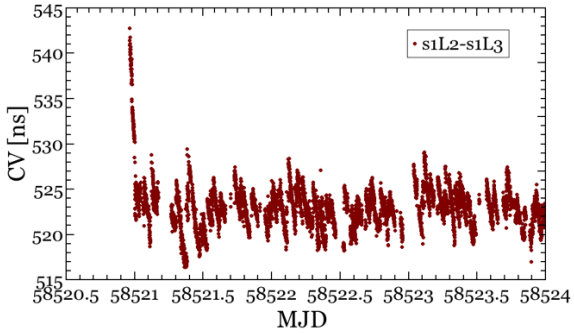

Fig. 7. CV between the second and the third sets of SDR data collected in December 2021 from the same scenario from the GSG64, a few ms arbitrary offset subtracted.

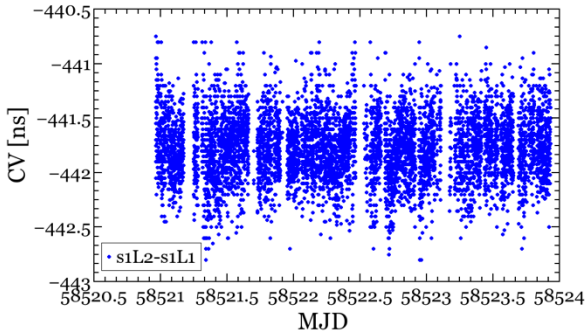

Fig. 8. CV between the first and the second sets of SDR data collected in December 2021 from the same scenario from the GSG64, a few ms arbitrary offset subtracted.

Nevertheless, the overall stability of the SDR CV, as estimated from a TDEV computation by neglecting gaps, and by suppressing the transient term at the beginning of the data set when appearing, are mostly at the ns level or just below. Figure 9 is showing the TDEV of SDR CV as shown on Figure 7, with the above-mentioned pattern in the data, but with the transient term withdrawn. The CV are computed between s1L2 and either s1L3 (data plotted in Figure 7) or s1L5 (the fifth set of data in December 2021), with a similar result. Obviously, the noise stays close to 1 ns over almost any analysis periods, indicating that some additional data filtering is required to get lower TDEV. Alternatively, Figure 10 is showing the TDEV of SDR CV as shown in Figure 8. Here, the CV are computed between s1L2 and either s1L3 (data plotted in Figure 8) or s1L4 (fourth set of data in December 2021), and between s1L3 and s1L5. Note that s1L4 data were obtained with a 10 dB higher power, but this does not seem to improve the noise. The best TDEV is obtained between s1L3 and s1L5, which means that the pattern visible on Figure 7 might be very similar if not the same in both datasets, hence cancelled by CV. In these cases, there is a largely sub-ns, and even sub-100 ps, noise reproducibility of the GPS simulated data collected by SDR, which is very encouraging for the next steps.

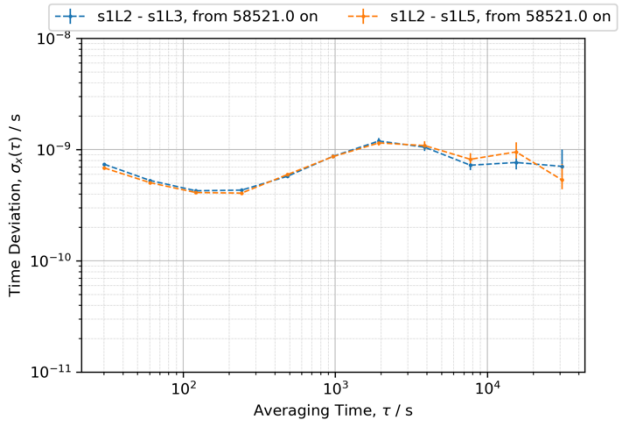

Fig. 9. TDEV of the CV between different series of SDR collected data, after withdrawing the transient term as appearing on Figure 7 at the beginning of the datasets.

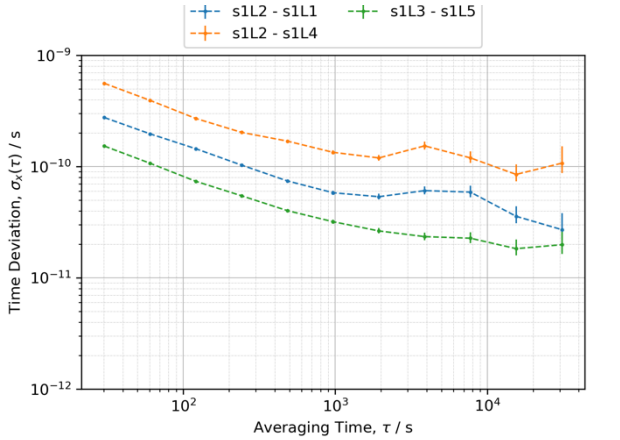

Fig. 10. TDEV of the CV between different series of SDR collected data. In the red plot, s1L4 data were obtained with a 10dB higher power compared to all other datasets.

A similar analysis was carried out between simulator and SDR generated RINEX files, after transformation into 30 s sampled CGGTTS files. Figure 11 shows a typical result of CV between the SDR file s1L3 already used above and one GSG64 file, named z1L3 according to: “z” for the simulator, “1” for 2021, “L” for December and “3” for third set of measurements. As for the plots above, a few ms arbitrary offset was withdrawn from the plotted data. One can see again some initial transient term, and the pattern already mentioned above, with some gaps in the data. In addition, there seem to be a trend in the CV and there is a jump of about 20 ns in the data set, for which we do not have any explanation. But we also see that there is about one third of the data set in the middle of the plot where the noise is significantly smaller. We still have to understand why and how these differences in data sets issued from one single scenario only.

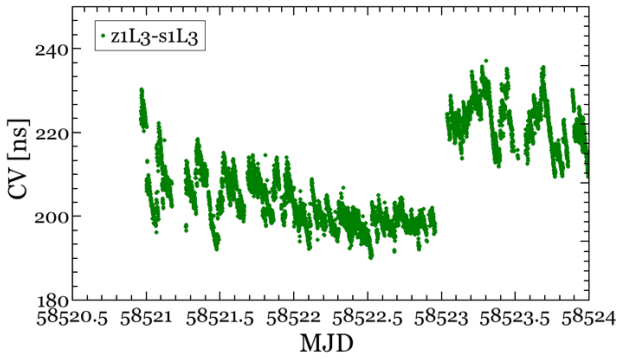

Fig. 11. CV between the third set of simulator and SDR files collected in December 2021, a few ms arbitrary offset subtracted.

Figure 12 is showing CV between z1L1 and s1L1 files, based on the first sets of measurements in December 2021, the best result so far. A few ms arbitrary offset was withdrawn from the plotted data. Again, the transient term is visible at the start, together with the pattern already seen elsewhere and some missing data. But the CV are looking steadier compared to the plot above.

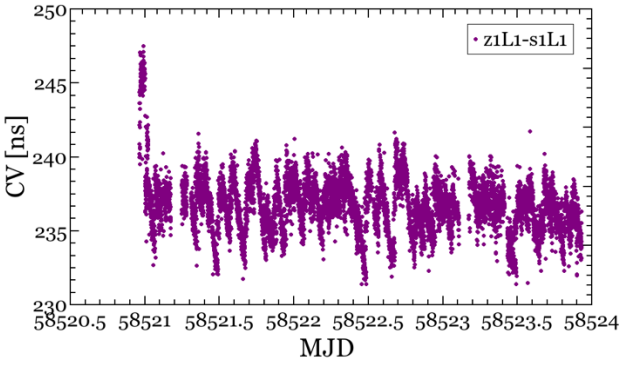

Fig. 12. CV between the first set of simulator and SDR files collected in December 2021, a few ms arbitrary offset subtracted.

A TDEV analysis is proposed on Figure 13. It is limited to series of data considered without the transient term at the start of the CV files and by neglecting gaps in the data. The CV are computed between z1L1 and s1L1 (plotted in Figure 12), between z1L2 and s1L2 (second sets of measurements in December 2021), and between z1L4 and s1L3 (fourth set of simulator data against third set of SDR data). We remind that all these data are based on the very same scenario at simulator level, but with potential differences in the initial synchronization on UTC(OP) 1 PPS. What can be noticed again is the fact that the TDEV sees the pattern present in the CV plot as a periodic term of about 5 000 s half-period. But on the other hand, the noise limit remains close to 1 ns, which is not good enough for a sub-ns level final uncertainty budget target yet.

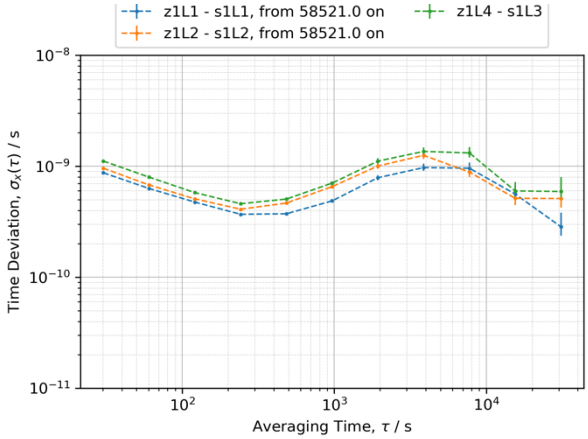

Fig. 13. TDEV of the CV between different series of simulator and SDR collected data. The common bump at an averaging period of about 5 000 s seems to be mostly due to the pattern present in the CV data.

V CONCLUSIONS

This paper is describing a work in progress, which was severely hampered during the last two years by the Covid-19 pandemic restrictions.

We have first shown how we obtained the limits we could achieve in measuring with an oscilloscope the offset between the reference 1 PPS signal and the simulated GNSS signal code transition with the equipment available in LNE-SYRTE. A sub-ns final uncertainty target was requiring additional bandpass filtering delays development with the use of a VNA. We proposed to consider a new approach based on the SDR technique.

We selected and implemented an SDR GNSS receiver, driven by the free software gnss-sdr. We limited our tests so far to a GPS L1 C/A simulated signal within one single 12 satellites scenario. The basic analysis was made on CV between 30 s sampled CGGTTS files issued from RINEX files. We noticed numerous issues in the measurement process, among others the initial synchronization on UTC(OP) 1 PPS, which was depending on the choice between a hardware “hold” button on the front end of the simulator or a remote software action via Studio View. When using the simulator 1 PPS output as the SDR receiver 1 PPS input, we also noticed that the start of SDR measurements was not reproducible, and that the resulting CV differences were varying from -0.4 ms to 9.7 ms. In some data sets, there is a transient term at the start of the measurements which had to be withdrawn before carrying out a TDEV analysis. In most of the CV, there is a pattern leading to a TDEV 1 ns bump for an averaging period of about 5 000 s. A coordinate issue was first suspected, but discarded as some of the CV datasets were not exhibiting the pattern when using the same

virtual antenna coordinates. And, last but not least, there were irregular gaps or jumps in the collected data, still unexplained too.

When comparing by CV the SDR files with each other, the best results were providing a TDEV below 100 ps for averaging periods above 300 s, showing an excellent reproducibility of the noise. This is a very encouraging result for a sub-ns final uncertainty target. When comparing by CV the simulator and the SDR files, the TDEV results were obviously limited to about 1 ns by the pattern we see in the data. More work is required to understand the source of this pattern, and to suppress it from the data. The next step would be to explain the ms differences between different series of measurements based on one single simulated scenario. In the future, similar developments would have to be carried out by using different GNSS codes and carriers.

ACKNOWLEDGMENT

We are grateful to G.D. Rovera, retired from LNE-SYRTE, for fruitful discussions. We acknowledge the authors of the gnss-sdr software for making it freely available. We thank P. Defraigne (ORB) for having distributed her RINEX to CGGTTS software freely.

DISCLAIMER

Product names and model numbers of the equipment are included for reference only. No endorsement or criticism is implied.

REFERENCES

1 J. Plumb, K. Larson, J. White and E. Powers "Absolute calibration of a geodetic time transfer system" IEEE Trans. Ultrason. Ferroelectr. Freq. Control ***52*** (2002)*1904–11*

2 E. Garbin *et al, "*Absolute calibration of GNSS timing stations and its applicability to real signals", *Metrologia* **56** (2019) 015010 https://doi.org/10.1088/1681-7575/aaf2bc

3 D. Valat and J. Delporte, "Absolute calibration of timing receiver chains at the nanosecond uncertainty level for GNSS time scales monitoring", *Metrologia* **57** (2020) 025019, https://doi.org/10.1088/1681-7575/ab57f5

4 P. Waller, R. Valceschini, J. Delporte and D. Valat, "Cross-calibrations of multi-GNSS receiver chains", Proc. of the Joint Meeting of the 2019 IEEE Frequency Control Symposium (IFCS) and of the 33rd European Frequency and Time Forum (EFTF), Orlando, Florida, USA, 2019.

5 G.D. Rovera, M. Abgrall, P. Uhrich and M. Siccardi, "Techniques of antenna cable delay measurement for GPS time transfer*"*, Proc. of the Joint Meeting of the 29th EFTF and of the 2015 IFCS, Boulder, USA, April 2015 pp 239-44.

6 G. Cibiel, A. Proia, L. Yaigre, J-F. Dutrey, A. de Latour and J. Dantepal "Absolute calibration of geodetic receivers for time transfer: electrical delay measurement, uncertainties and sensitivities" Proc. of the 22nd EFTF, Toulouse, France, 2008.

7 J. Delporte, D. Valat, T. Junique and F-X. Marmet, "Progress on absolute calibrations of GNSS reception chains at CNES", Proc. of the 2016 IFCS, New Orleans, USA, April 2016
https://doi. org/10.1109/FCS.2016.7546776.

8 Z. Jiang *et al.*, "Use of software-defined radio receivers in two-way satellite time and frequency transfers for UTC computation." *Metrologia.* **55** (2018) https://doi.org/10.1088/1681-7575/aacbe6

9 G.D. Rovera, S. Bize, B. Chupin, J. Guéna, Ph. Laurent, P. Rosenbusch, P. Uhrich and M. Abgrall, "UTC(OP) based on LNE-SYRTE Primary Frequency Standards", *Metrologia* **53** (2016) S81-S88.

10 URL: https://gnss-sdr.org